(OH)(H_2)-$_n$, 137332-68-4; -(N(CH_2Ph)C_6H_4-p-CH_2-C_6H_4-p-N(CH_2Ph)CH_2CH(OH)CH_2OCOCH_2COOCH_2CH(OH)CH_2)-$_n$, 137332-69-5; -(N(CH_2Ph)C_6H_4-p-CH_2-C_6H_4-p-N(CH_2Ph)CH_2CH(OH)CH_2OCO(CH_2)$_2$COOCH_2CH(OH)CH_2)-$_n$, 137332-70-8; -(N(CH_2Ph)C_6H_4-p-CH_2-C_6H_4-p-N(CH_2Ph)CH_2CH(OH)-CH_2OCO(CH_2)$_3$COOCH_2CH(OH)CH_2)-$_n$, 137332-71-9; -(N-(CH_2Ph)C_6H_4-p-CH_2-C_6H_4-p-N(CH_2Ph)CH_2CH(OH)-CH_2OCOCH=CHCOOCH_2CH(OH)CH_2)-$_n$, 137332-72-0; CBr_4, 558-13-4; bis(oxioyl)-1,2,2-trimethyl-1,3-cyclopentanedicarboxylate, 74567-40-1; bis(oxioyl)-4-methyl-4-cyclohexene-1,2-dicarboxylate, 137332-66-2; N,N'-dibenzyl-N,N'-bis(2,3-epoxypropil)-4,4'-diaminodiphenylmethane, 130036-13-4; oxalic acid, 144-62-7; malonic acid, 141-82-2; amber acid, 110-15-6; glutaric acid, 110-94-1; maleic acid, 110-16-7.

Surface Chemistry of Sulfidized Mercury Cadmium Telluride As Probed by Voltammetry and Photoelectrochemistry

Chang Wei, Kamal K. Mishra, and Krishnan Rajeshwar*

Department of Chemistry, Box 19065, The University of Texas at Arlington, Arlington, Texas 76019-0065

Received June 19, 1991. Revised Manuscript Received September 20, 1991

The sulfidation of mercury cadmium telluride (MCT) single crystal surfaces was studied by cyclic/linear sweep voltammetry and photoelectrochemical techniques. The study was done mainly in aqueous polysulfide solutions, although a brief comparison witn nonaqueous ethylene glycol medium is also provided, particularly with respect to oxide contamination. The evolution of the surface composition with the electrode potential was mapped by using (a) reference voltammograms for sulfidized Hg and Te surfaces along with the voltammetric behavior of polysulfide solutions at Pt, (b) linear sweep photovoltammetry, combining wavelength-selective light excitation with voltammetric scanning of the MCT surface in polysulfide, and (c) photocurrent spectroscopy (i_{ph} vs λ) at selected potentials. With these data as a unit, it is shown that CdS forms first on sulfidation of MCT followed by HgS in two stages. Subsequently, the polysulfide solution undergoes oxidation to elemental sulfur at the MCT surface along with partial oxidation of Hg to HgO (the latter only in aqueous media). At higher potentials, HgS dissolves as HgS_2^{2-}, and Te sulfidizes to TeS_2 followed by its dissolution as TeS_3^{2-}. The last stage (again only in aqueous media) comprises the generation of higher oxidation states of Te^{4+} (as TeO_x) and S^0. At positive potentials, the net result of the sulfidation is the formation of Cd-rich MCT (contrasting with the starting composition, $Hg_{0.8}Cd_{0.2}Te$). Supportive data from X-ray photoelectron spectroscopy and differential scanning calorimetry are also presented.

Introduction

Mercury cadmium telluride (MCT, $Hg_{1-x}Cd_xTe$, $x \simeq 0.2$–0.3) is a key material component of infrared systems research and technology. Since its electrical properties are dominated by surface recombination velocity, much attention has focused in recent years on strategies for passivating the surface. Anodic sulfidation of MCT has been proposed as a second-generation passivation tool by Nemirovsky and co-workers.[1-3] The earlier contention by these authors that the sulfidized surface comprised predominantly CdS has not been borne out by later studies[4,5] which have shown the presence also of significant quantities of S, Hg, and Te at the surface. The sulfidation has been carried out (predominantly by galvanostatic methods) both in nonaqueous solvents (ethylene glycol)[1-5] and in aqueous media.[6] Differences have been reported in the type of surface layers that are formed in the two cases.[6]

In spite of the fact that an electrochemical technique is employed for the sulfidation of MCT, systematic characterization of the resultant surfaces using voltammetry has not been performed. In previous studies in this laboratory,[7,10] we have shown how the information content of this powerful analytical tool is considerably enhanced by combining it with light excitation especially for photoresponsive electrode materials such as semiconductors. Thus, the primary objective of this report is to describe the voltammetric and photoelectrochemical characterization of MCT surfaces in polysulfide solutions. To probe the evolution of the surface chemistry as a function of potential, we employed a potentiostatic analysis mode, contrasting with the earlier studies.[1-6] We show that CdS forms first on the MCT surface followed by the sulfidation of the Hg and Te components at higher potentials. Finally, the dissolution of Hg and Te sulfides leaves a Cd-rich MCT surface. A brief comparison of the surface chemistry, particularly from the point of view of oxide contamination, was also performed for aqueous vs nonaqueous sulfidation media.

Experimental Section

Electrodes and Chemicals. Single crystals of MCT of nominal composition, $Hg_{0.8}Cd_{0.2}Te$, were donated by Texas Instruments, Inc. These crystals were n-type with a carrier concentration of $\sim 10^{15}$ cm^{-3}. Indium was used as the ohmic contact, and a Cu

* Author for correspondence.

(1) Nemirovsky, Y.; Burstein, L. *Appl. Phys. Lett.* **1984**, *44*, 443.
(2) Nemirovsky, Y.; Burstein, L.; Kidron, I. *J. Appl. Phys.* **1985**, *58*, 366.
(3) Nemirovsky, Y.; Adar, R.; Kornfield, A.; Kidron, I. *J. Vac. Sci. Technol.* **1986**, *A4*, 1986.
(4) Strong, R. L.; Luttmer, J. D.; Little, D. D.; Teherani, T. H.; Helms, C. R. *J. Vac. Sci. Technol.* **1987**, *A5*, 3207.
(5) Ippõshi, I.; Takita, K.; Murakami, K.; Masuda, K.; Kudo, H.; Seki, S. *J. Appl. Phys.* **1988**, *63*, 132.
(6) Ziegler, J. P.; Lindquist, J. M.; Hemminger, J. C. *J. Vac. Sci. Technol.* **1989**, *A7*, 469.
(7) Mishra, K. K.; Rajeshwar, K. *J. Electroanal. Chem.* **1989**, *271*, 279.
(8) Mishra, K. K.; Rajeshwar, K. *J. Electroanal. Chem.* **1989**, *273*, 169.
(9) Ham, D.; Mishra, K. K.; Weiss, A.; Rajeshwar, K. *Chem. Mater.* **1989**, *1*, 619.
(10) Rajeshwar, K. *Adv. Mater.*, in press.

0897-4756/92/2804-0077$03.00/0

lead was attached to it using conducting epoxy (Johnson Mathey Electronics). Insulating epoxy was used to encase the electrode and delineate the area exposed to the electrolyte. Prior to use, the MCT surface was polished with Al_2O_3 (Buehler) down to 0.05 μm followed by cleaning with acetone and deionized water. Some experiments also utilized Hg and Te thin-film working electrodes. These films were cathodically electrodeposited at glassy carbon or Pt substrate electrodes according to procedures described elsewhere.[11]

A standard three-electrode, single-compartment cell design was employed for the electrochemical and photoelectrochemical experiments. A Pt spiral served on the counterelectrode, and Ag/AgCl was employed as reference. All potentials are quoted with respect to this electrode unless specified otherwise. All measurements were performed at 22 ± 0.5 °C on carefully deoxygenated solutions.

All chemicals were from commercial sources and used as received. *Caution*: Adequate precautions need to be taken in the handling and disposal of Hg-, Cd-, and Te-containing solutions.

Instrumentation. Electrochemical experiments utilized either an EG&G Princeton Applied Research (PAR) Model 273 system of a PAR Model 173 potentiostat/galvanostat equipped with PAR Model 175 and Model 179 modules. Photoelectrochemical experiments additionally used a Spectrodata SD90 (Aries Instruments) Ebert 250-mm monochromator and a quartz tungsten halogen light source. An EG&G Model 5208 two-channel lock-in amplifier was used in conjunction with an EG&G Model 194A light chopper to separate the photocurrents from the dark current component. A Perkin-Elmer Model 5000C system (Physical Electronics) was used for XPS. Al Kα radiation (1486.6 eV) was employed as the X-ray source. Depth profiles were acquired with 4-keV Ar^+ ion sputtering. Differential scanning calorimetry (DSC) utilized a Du Pont 9900 thermal analysis system fitted with a Model 910 accessory module. Sealed Al pans and a dynamic N_2 atmosphere were employed according to procedures detailed elsewhere.[12] A heating rate of 15 °C/min was employed.

Results and Discussion

Sulfidation Chemistry and Electrochemistry. Background. Polysulfide solutions were prepared in this study using either 1 M NaOH (for aqueous media) or ethylene glycol (for the nonaqueous portion of the study). The dominant sulfur solution species in either case are HS^- and S_3^{2-}, although only aqueous media appear to be well characterized.[13] As pointed out by other authors,[6] thermodynamic data also are sparse for the ethylene glycol case. Therefore, the following discussion pertains largely to aqueous solutions.

As with the anodic oxidation counterpart, chemistry and electrochemistry are intimately coupled at the MCT/electrolyte interphase—the latter involving the oxidation of the components at the solid phase and the former leading to precipitation of the cations thus generated with the sulfide anions from the solution part of the interphase. The stability of the resultant surface layers will be determined largely by their solubility product and complexation equilibria.

The predominance of CdS at sulfidized MCT surfaces as initially claimed by Nemirovsky et al.[2] thus was based on the following chemistry:

$$CdS = Cd^{2+} + S^{2-} \qquad K = 1.0 \times 10^{-28} \qquad (1)$$

$$HgS + S^{2-} = HgS_2^{2-} \qquad K = 1.8 \qquad (2)$$

$$TeS_2 + S^{2-} = TeS_3^{2-} \qquad K = 4.1 \times 10^{7} \qquad (3)$$

That is, CdS is very stable in polysulfide media whereas the sulfides of Hg and Te form (soluble) complexes. The equilibrium constants quoted above are from refs 2 and 14.

Table I. Pertinent Electrochemical Reactions and the Associated Redox Potentials in the MCT/Polysulfide System

reaction	redox potential, V vs Ag/AgCl
$Cd + S^{2-} = CdS + 2e$	−1.38
$Hg + S^{2-} = HgS + 2e$	−0.87
$S^{2-} = S^0 + 2e$	−0.65
$Te + 2S^{2-} + TeS_2 + 4e$	−0.64[a]

[a] Since the standard potential for this reaction is not available to our knowledge, the quoted potential is computed using thermodynamic data, and the standard potential known for the reaction: $TeS_3^{2-} + 4e = Te^0 + 3S^{2-}$ (−0.56 V vs SHE) from ref 14. All the other potentials are from ref 15.

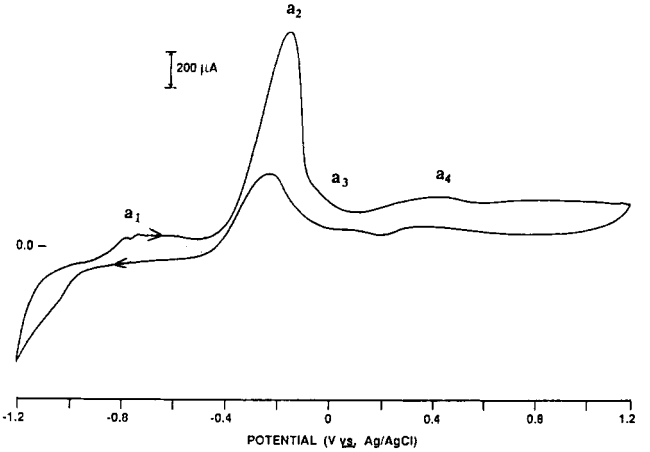

Figure 1. Representative cyclic voltammogram for a $Hg_{0.8}Cd_{0.2}Te$ crystal in 0.1 M Na_2S/1 M NaOH. The potential scan rate was 20 mV/s.

The overall anodic sulfidation of MCT is well represented by eq 4 for the composition ($x = 0.2$) specific to this study:[2,6]

$$Hg_{0.8}Cd_{0.2}Te + 1.8HS^- + S_3^{2-} + 1.8OH^- = 0.2CdS + 0.8HgS_2^{2-} + TeS_3^{2-} + 1.8H_2O + 2e^- \qquad (4)$$

It must be noted that the complications due to competing oxide generating reactions in aqueous media (Cd → CdO, Hg → HgO, Te → TeO_x, etc.) have not been considered here in this synopsis. (However, see below.)

Table I contains a glossary of the pertinent electrochemical reactions and the associated redox potentials.

Linear Sweep Voltammetry. Voltammetric data on the sulfidation of MCT are confined, to our knowledge, to a brief examination by Ziegler et al.[6] These authors observed three anodic peaks at −0.28, −0.05, and +0.30 V (vs SCE) for $Hg_{0.7}Cd_{0.3}Te$ in aqueous polysulfide and assigned them to Cd, Hg, and Te sulfidation, respectively. Further, large background current flow was observed between −0.5 and 0 V (vs SCE) and attributed to solution oxidation reactions. The anodic sulfidation of Hg and Cd electrodes has been studied in detail by previous authors.[16,17] With these studies as background, we now proceed to describe our voltammetric findings.

Figure 1 contains a representative cyclic voltammogram for MCT in 0.1 M aqueous polysulfide. Four anodic current flow regimes (labeled a_1–a_4) are identifiable; the

(11) Mori, E.; Mishra, K. K.; Rajeshwar, K. *J. Electrochem. Soc.* **1990**, *137*, 1100.
(12) Lin, W.-Y.; Mishra, K. K.; Mori, E.; Rajeshwar, K. *Anal. Chem.* **1990**, *62*, 821.
(13) Hodes, G.; Miller, B. *J. Electrochem. Soc.* **1986**, *133*, 2177.
(14) *Gmelin Handbuch der Anorganisachen Chemie, Tellur, Ergänzungsband, B3*; Springer-Verlag: Berlin, 1983.
(15) Antelman, M. S. *The Encyclopaedia of Chemical Electrode Potentials*; Plenum: New York, 1982.
(16) Peter, L. M.; Reid, J. D.; Scharifker, B. R. *J. Electroanal. Chem.* **1981**, *119*, 73.
(17) Peter, L. M. *Electrochim. Acta* **1978**, *23*, 165.

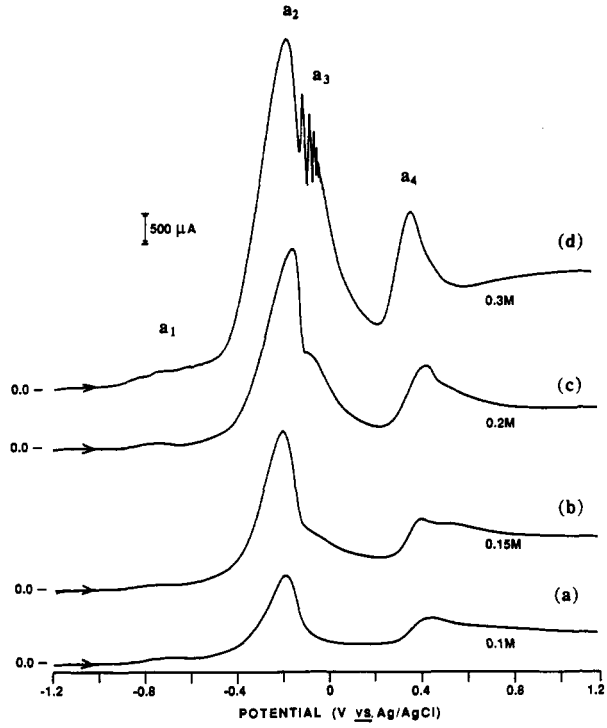

Figure 2. Linear sweep voltammograms for a $Hg_{0.8}Cd_{0.2}Te$ crystal in 1 M NaOH containing the indicated Na_2S concentration. Note that the voltammetric trace in Figure 2a is similar to that contained in Figure 1 except that the current sensitivity is lower. Other scan conditions as in Figure 1.

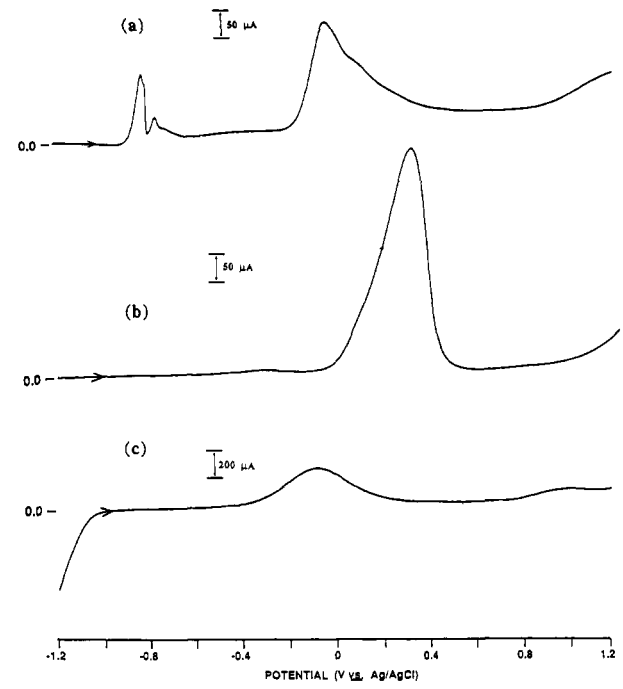

Figure 3. Linear sweep voltammograms for electrodeposited thin films of Hg (Figure 3a), Te (Figure 3b), and for a Pt working electrode (Figure 3c) in 0.1 M Na_2S/1 M NaOH. Scan conditions as in Figure 1.

evolution of these with increasing polysulfide concentrations is illustrated in Figure 2. As an aid to interpreting these voltammetric features, the sulfidation of Hg and Te and the oxidation of polysulfide at Pt was considered; the respective "reference" voltammograms are contained in Figure 3. In comparing the two sets of data in Figures 1 and 3, it has to be borne in mind that the initial species are present in different oxidation states in the two instances. That is, Hg and Te are in the ionized form in MCT while they are initially in the (native) zero oxidation state in the experiments in Figure 3.

The response of a_3 to the polysulfide concentration (Figure 2) enables its assignment to polysulfide (solution) oxidation at the MCT surface. Indeed, there is good match of the reference peak in Figure 3c with a_3. The assignment of a_1 to (monolayer) HgS formation[16,17] also appears to be straightforward based on the voltammogram in Figure 3a. On thermodynamic grounds, bulk HgS formation would be expected to be more facile in the ionic (MCT) state relative to the native Hg^0 form. Indeed, a_2 is shifted to a negative potential relative to the major feature in the voltammogram in Figure 3a, so much so that a_2 now overlaps with the polysulfide oxidation wave (Figure 3c). Conversely, sulfidation of Te in MCT (formal oxidation state of Te, −2) should be less favored relative to the Te^0 state. This trend is realized experimentally: compare a_4 with Figure 3b. The current flow at potentials more positive than ~0.6 V in Figure 1 is attributed to the oxidation of both Te^{4+} and S^0 to higher oxidation states (cf. Figure 3b,c and also FIgure 2d). In summary, we assign a_1 and a_2 in Figure 1 to HgS formation, a_3 to polysulfide oxidation, and a_4 to Te sulfidation.

While our voltammograms broadly resemble the one reported by Ziegler et al.[6] (except for the resolution of a greater number of anodic waves in ours), our interpretation (which is based on extensive reference voltammetry data) is clearly at variance with theirs, especially with respect to the Cd- and Hg-related features. We consistently fail to observe Cd-related waves in our voltammograms. On the basis of previous work[9,17] both in this laboratory and elsewhere, we would have expected these to occur at potentials negative of ~−1.0 V. (A positive shift due to compound stabilization, however, is possible analogous to the Hg case discussed above.) It is possible that our failure to observe CdS formation is, partly at least, because of two factors: (a) the cathodic current flow at these potentials (cf. Figure 1) obscures the Cd sulfidation wave; (b) the sensitivity is inadequate at the low Cd content (x = ~0.2) of our MCT samples. However, we do detect CdS via linear sweep photovoltammetry (cf. Figure 5b). Further support for our assignment of a_2 to HgS formation is also provided by the linear sweep photovoltammetry data presented below. Additionally, we will show further evidence from DSC later for the formation of elemental S^0 at the MCT surface.

When a slow potential scan rate (e.g., 2 mV/s) is employed, a shoulder is observed on the polysulfide oxidation wave (Figure 4a). We assign this to the oxidation of Hg to HgO[11]—an interpretation which is also supported by the absence of this wave in ethylene glycol medium (Figure 4b). Further confirmation comes from the concomitant photoresponse at 550 nm (vide infra). (HgO is a semiconductor with a bandgap of ~1.9 eV; cf. ref 18). A linear sweep voltammetric scan of a Hg film in NaOH (in the absence of sulfide) shows a match of this shoulder with the sharp oxidation wave observed for HgO formation in the former case. This rules out Te oxidation as the origin of this shoulder (cf. Figure 3b). Interestingly enough, a further comparison of parts a and b of Figure 4 reveals the absence of anodic current flow at potentials greater than ~0.6 V in the nonaqueous medium. This provides confirmation of our original assignment of this regime to the generation of higher oxidation states of Te^{4+} and S^0 in aqueous media (cf. Figures 2 and 3). Thus, the sulfidation

(18) DaSilva Pereira, M. I.; Peter, L. M. *J. Electroanal. Chem.* **1982**, *131*, 167.

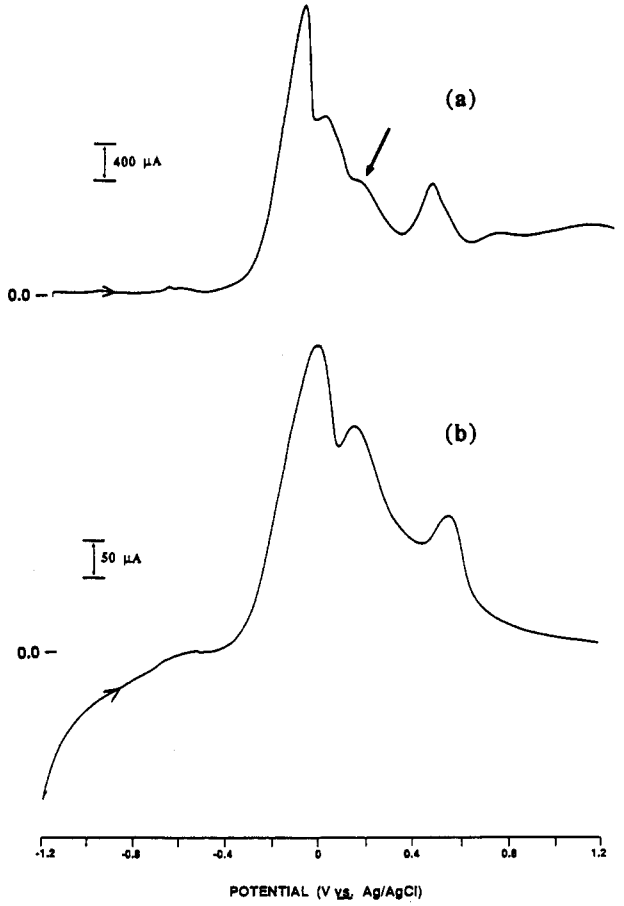

Figure 4. Representative linear sweep voltammograms for $Hg_{0.8}Cd_{0.2}Te$ crystal in 0.1 M Na_2S/1 M NaOH (Figure 4a) and 0.1 M Na_2S/ethylene glycol (Figure 4b). The potential scan rate was 2 and 5 mV/s in (a) and (b), respectively.

of MCT in aqueous media is accompanied also by the generation of HgO and TeO_x. We have no evidence from voltammetry for the generation of CdO. This process has been studied by us earlier in polysulfide media albeit at Cd-containing surfaces other than MCT.[9,19]

Returning to Figure 1, the observation of *anodic* waves on the negative-going scan is worthy of note. This indicates (as pointed out by a reviewer) that a_3 blocks further progress of Hg sulfidation on the forward scan. When soluble species (e.g., HgS_2^{2-}, TeS^{3-}, higher oxidation states of S^0) are subsequently generated at more positive potentials than a_3 on the forward scan, fresh surfaces are exposed such that a_2 occurs again on the return cycle.

Photoelectrochemistry. Parts a and b of Figure 5 contain representative linear sweep photovoltammograms, acquired with lock-in detection (cf. the Experimental Section), at two excitation wavelengths, 550 and 430 nm, respectively. The major difference between these scans is the clear presence of a photoactive phase at potentials below ~−0.2 V in Figure 5b but *not* in Figure 5a. CdS is photoexcited at 430 nm but not at 550 nm (bandgap energy = 2.4 eV ≡ ~516 nm). The photoactivity at potentials greater than ~−0.2 V in Figure 5 is attributable to HgS, HgO, and MCT itself (see below). It is interesting that the photoanodic current flow shows dips and valleys. The initial dip in the photocurrent is attributable to the deposition of a (nonphotoactive) S^0 overlayer. Subsequently, the photoactivity rises again because of the formation of HgO. The loss of HgS as HgS_2^{2-} (cf. eq 2) causes a diminution of the photoactivity. The photoresponse stabilizes at potentials greater than ~0.5 V, signalling that these processes have ceased to play an important role (or at least have reached a steady state).

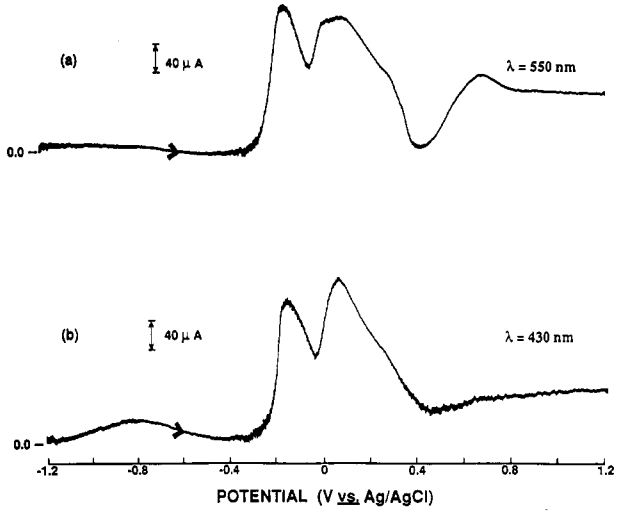

Figure 5. Linear sweep photovoltammograms for a $Hg_{0.8}Cd_{0.2}Te$ crystal (potential scan rate 2 mV/s) in 0.1 M Na_2S/1 M NaOH. The excitation wavelength was 550 and 430 nm in (a) and (b) respectively, and the photocurrents were measured with lock-in detection.

Delineation of the photoactive components is possible via photocurrent spectroscopy. This was done at selected potentials along the voltammetry profile in Figure 1. Three such i_{ph}–λ scans are shown in Figure 6; the analyses of these data in terms of the Stern expression[20]

$$i_{ph} = k(h\nu - E_g)^{n/2}/h\nu \qquad (5)$$

are contained in Figure 7. In eq 5, i_{ph} is the photocurrent, E_g is the bandgap energy, k is a constant, and the exponent is either 1 or 4 depending on whether the semiconductor bandgap is direct or indirect, respectively.

At −0.6 V, the main component at the MCT surface is expected to be CdS (although this potential occurs close to the monolayer HgS wave, a_1 (cf. Figure 1),[16] the perturbation from HgS will be minimal until potentials into the bulk HgS formation wave, a_2, are accessed). Indeed, Figures 6a and 7a yield a bandgap for the photoactive phase of ~2.4 eV—close to that characteristic of CdS. Similarly, analyses of Figures 6b and 7b identify the photoactive phase to be HgS (bandgap energy = 1.92 eV[21]). Finally, the dissolution of HgS and TeS_2 from the MCT surface (reactions 2 and 3) leaves a Cd-rich MCT surface which yields a bandgap energy of 1.5 eV (cf. Figures 6c and 7c). The latter value is actually close to that of CdTe.

The linear sweep photovoltammetry and photocurrent spectroscopy data thus provide an internally consistent framework for the voltammetry interpretation presented in the preceding section.

X-ray Photoelectron Spectroscopy. The survey spectra of the sulfidized MCT samples (not shown) revealed the expected Cd, Hg, Te, and S signals in addition to C, O, and Na. Semiquantitative analyses were performed at samples sulfidized at −0.6 and 1.2 V. Consistent with the findings summarized earlier, the Cd levels were significantly higher at 1.2 V relative to −0.6 V (~48 at. % vs 8 at. %). Although the quantitation of Hg via high-

(19) Ham, D.; Son, Y.; Mishra, K. K.; Rajeshwar, K. *J. Electroanal. Chem.* **1991**, *310*, 417.

(20) Stern, F. *Solid State Phys.* **1963**, *15*, 299.

(21) Abrikosov, N. K.; Bankina, V. F.; Poretskya, L. V.; Shelimova, L. E.; Skudnova, E. V. *Semiconducting II-VI, IV-VI* and *V-VI Compounds*; Plenum: New York, 1969.

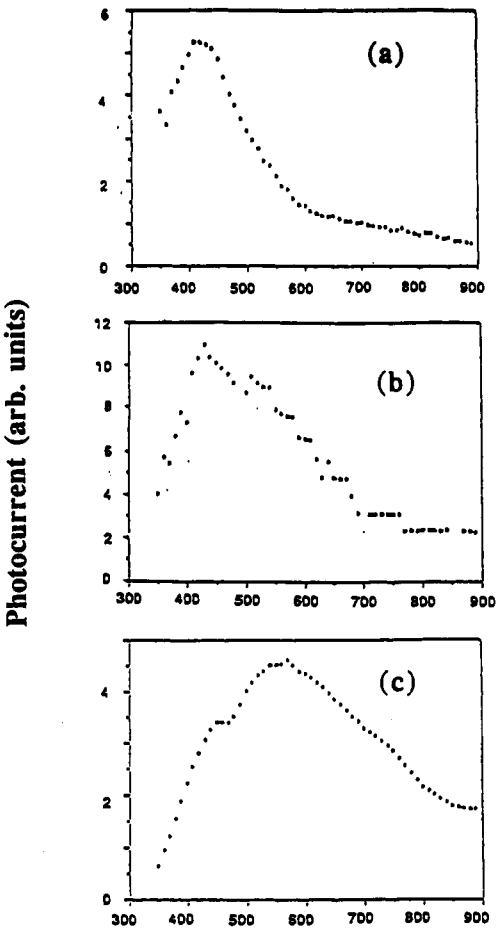

Figure 6. Photoaction spectra of a $Hg_{0.8}Cd_{0.2}Te$ crystal in 0.1 M Na_2S/1 M NaOH at −0.60 V (a), −0.1 V (b), and 1.2 V (c).

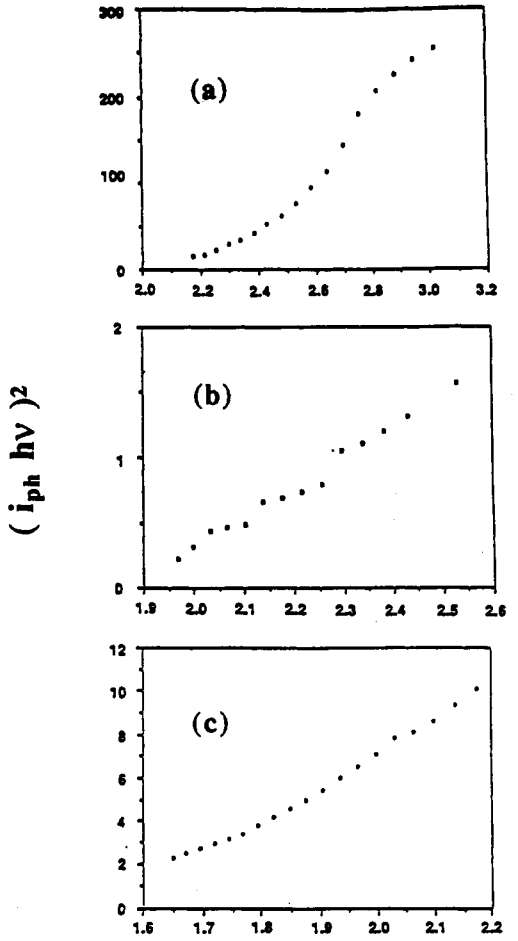

Figure 7. Analyses of the data in Figure 6 according to eq 5 (refer to text). The exponent, n, was taken to be 1 as appropriate to a direct-gap semiconductor. Panels a–c correspond in Figures 6 and 7.

vacuum techniques is fraught with uncertainty because of its high volatility, the Hg/Cd ratio appears to switch from ~4 in the starting material to ~$^1/_4$ (i.e., by a factor of 16) on sulfidation at 1.2 V.

Differential Scanning Calorimetry. We have shown earlier[12] how DSC could play a useful role in semiconductor thin-film characterization. Figure 8 contains a DSC trace of an anodic surface film sample obtained from the sulfidation of MCT in 0.1 M Na_2S at 0.8 V. This sample was scraped off from the MCT surface and then scanned in the DSC cell. The endotherm at 113.2 °C is in excellent agreement with the melting signature for rhombic sulfur reported by a previous author.[22] Figure 9 provides another example wherein we have found DSC to be useful in the elucidation of MCT surface chemistry. This trace was obtained for an anodic surface film sample from another MCT crystal passivated in 0.1 M KOH at 1.0 V. (The sample was prepared for the DSC run as before.) A sharp exotherm at ~55 °C is observed. As discussed by Strong et al.,[4] reactions 6 and 7 involving the oxidation are both

$$HgTeO_3 + CdTe \rightarrow CdTeO_3 + HgTe \quad (6)$$

$$3TeO_2 + 2CdTe \rightarrow 2CdTeO_3 + 3Te \quad (7)$$

exothermic by 36 and 25 kcal, respectively. Thus while it is generally accepted that the anodic oxide begins to degrade around 65 °C, the data in Figure 9 provide *direct*

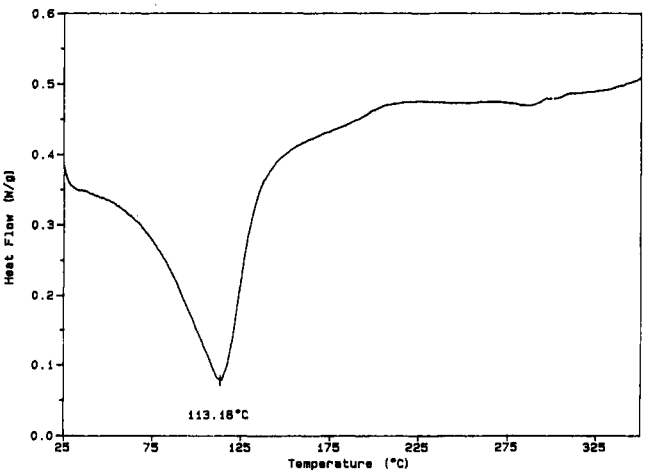

Figure 8. DSC thermogram (heating rate 15 °C/min) of an anodic surface layer. The sample was scraped from a sulfidized MCT surface (refer to text).

experimental support for the thermodynamic expectations.

Summary and Conclusions

We believe that we have provided a reasonable rationalization for the variance between the surface composition reported by previous authors[2-6] for sulfidized MCT sur-

(22) Chiu, J. *Anal. Chem.* **1963**, *35*, 933.

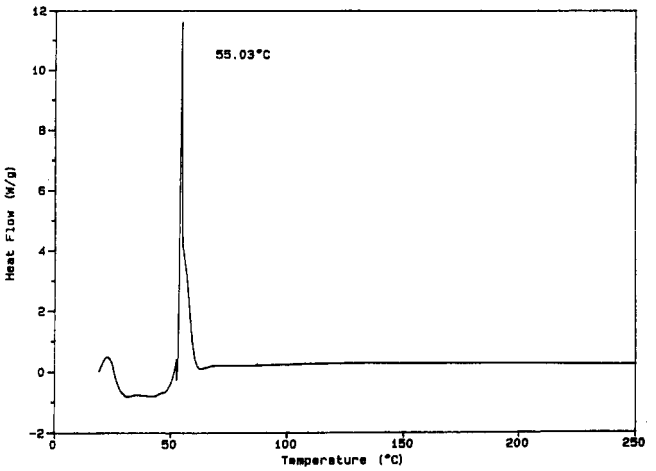

Figure 9. DSC thermogram (heating rate 15 °C/min) of an anodic surface oxide layer. The sample was scraped from a KOH-treated MCT surface (refer to text).

faces. For example, the Auger depth profiles presented in refs 2 and 3 on two different MCT samples show the peak-to-peak signal for Cd and S to be exactly opposite to the trend seen in two other more recent studies.[4,6] This discrepancy may be reconciled in light of this study, especially when it is noted that *both* CdS and S^0 contribute to the total sulfur content. Similarly, the origin of Cd lies with both MCT and CdS. Depending on the anodization time (i.e., potential) in the galvanostatic sulfidation employed in previous studies, the Cd/S ratio is likely to switch from >1 to a value <1 depending on whether S^0 formation or HgS/TeS_2 dissolution predominates. We have shown herein how the surface chemistry clearly is dependent on the sulfidization potential. At potentials lower than ~0.4 V (under the conditions pertaining to this study), the sulfidized MCT surface comprises mainly CdS; at potentials between ~0.4 and ~0.2 V, significant amounts of HgS and S^0 (along with some HgO in the case of aqueous media) are to be expected. At potentials more positive than ~0.8 V, a Cd-rich MCT surface results from the leaching of HgS and TeS_2. A puzzle not addressed in this study concerns the intriguing discrepancy between the observed and accepted value for the refractive index of CdS[4,6] and the claim[6] that two distinct forms of this material are obtained in aqueous vs nonaqueous sulfidation media. These and other issues related to the surface chemistry and electrochemistry of the passivation of MCT are being examined in this laboratory.

Acknowledgment. This research was supported, in part, by a grant from the Texas Higher Education Coordinating Board, Advanced Technology Program. We thank J. D. Luttmer of Texas Instruments, Inc., for the MCT crystals used in this study and for several discussions.

Registry No. $Hg_{0.8}Cd_{0.2}Te$, 39343-27-6; Na_2S, 1313-82-2; NaOH, 1310-73-2; CdS, 1306-23-6; HgS, 1344-48-5; HgS_2^{2-}, 26015-93-0; TeS_2, 7446-35-7; TeS_3^{2-}, 12300-21-9; S, 7704-34-9; HgO, 21908-53-2; Te, 13494-80-9; ethylene glycol, 107-21-1.

Isomorphous Substitution in $KTiOPO_4$: A Single-Crystal Diffraction Study of Members of the $K_{1-x}Na_xTiOPO_4$ Solid Solution

S. J. Crennell,† R. E. Morris,† A. K. Cheetham,† and R. H. Jarman*,‡

University of Oxford, Chemical Crystallography Laboratory, 9 Parks Rd., Oxford, OX1 3PD, U.K., and Amoco Research Center, P.O. Box 3011, Naperville, Illinois 60566

Received June 19, 1991. Revised Manuscript Received October 22, 1991

$K_{0.42}Na_{0.58}TiOPO_4$ was prepared by sodium ion exchange into $KTiOPO_4$ at 350 °C. Crystal data: orthorhombic, $Pn2_1a(33)$, a = 12.7298 (21), b = 10.6073 (13), c = 6.3074 (4) Å, V = 851.7 Å^3, Z = 4, D_c = 2.942 g cm^{-3}, $F(000)$ = 736. A sample was subsequently annealed at 700 °C. The structure of the ion-exchanged material is very similar to that found after annealing and is also consistent with that obtained in an earlier powder diffraction and solid-state NMR study of $K_{0.5}Na_{0.5}TiOPO_4$, confirming the validity of the powder work. There is considerable ordering over the two sites (site 1 0.933 (1) Na:0.067 (1) K; site 2 0.773 (7) K:0.227 (7) Na), and the single-crystal diffraction data are of sufficient resolution to detect the differing positions for the two cations on each site. Cation substitution does not affect the surrounding oxygen coordination sphere.

Introduction

The excellent nonlinear optical properties of $KTiOPO_4$ (KTP) have made it an important material for the second harmonic generation from the 1.06-μm radiation of Nd:YAG lasers.[1] Its structure[2] consists of chains in alternating TiO_6 octahedra and PO_4 tetrahedra parallel to the a and b axes, linked by helices of TiO_6 octahedra along [011] and [0$\bar{1}$1]. The octahedra in these helices are alternately cis and trans vertex sharing, building up a long–short–long chain of Ti–O bonds which is thought to be responsible for the large nonlinear coefficients of this material. The cations sit in channels running parallel to [100] and [001] with distorted hexagonal rings of oxygen atoms defining the windows between sites. All of the atoms in the structure are on general positions, making the structure very versatile with respect to isomorphous substitution:

† University of Oxford.
‡ Amoco Research Center.

(1) Bierlein, J. D.; Arweiler, C. B. *Appl. Phys. Lett.* **1986**, *49*, 917.
(2) Tordjman, I.; Masse, R.; Guitel, J. C. *Z. Kristallogr.* **1974**, *134*, 103.

0897-4756/92/2804-0082$03.00/0